IJC
International Journal of Cancer

Combined DNA methylation and gene expression profiling in gastrointestinal stromal tumors reveals hypomethylation of *SPP1* as an independent prognostic factor

Florian Haller[1], Jitao David Zhang[2], Evgeny A. Moskalev[1], Alexander Braun[3], Claudia Otto[3], Helene Geddert[4], Yasser Riazalhosseini[5], Aoife Ward[2], Aleksandra Balwierz[2], Inga-Marie Schaefer[6], Silke Cameron[7], B. Michael Ghadimi[8], Abbas Agaimy[1], Jonathan A. Fletcher[9], Jörg Hoheisel[5], Arndt Hartmann[1], Martin Werner[3], Stefan Wiemann[2,10] and Özgür Sahin[2]

[1] Institute of Pathology, Friedrich Alexander University, Erlangen-Nuremberg, Germany
[2] Division of Molecular Genome Analysis, German Cancer Research Center, Heidelberg, Germany
[3] Institute of Pathology, Albert Ludwigs University, Freiburg, Germany
[4] Institute of Pathology, St. Vincentius Hospital, Karlsruhe, Germany
[5] Division of Functional Genome Analysis, German Cancer Research Center, Heidelberg, Germany
[6] Institute of Pathology, Georg August University, Göttingen, Germany
[7] Department of Gastroenterology and Endocrinology, Georg August University, Göttingen, Germany
[8] Department of General and Visceral Surgery, Georg August University, Göttingen, Germany
[9] Department of Pathology, Brigham and Women's Hospital, Boston, MA
[10] Genomics and Proteomics Core Facility, German Cancer Research Center, Heidelberg, Germany

Cancer Cell Biology

Gastrointestinal stromal tumors (GISTs) have distinct gene expression patterns according to localization, genotype and aggressiveness. DNA methylation at CpG dinucleotides is an important mechanism for regulation of gene expression. We performed targeted DNA methylation analysis of 1.505 CpG loci in 807 cancer-related genes in a cohort of 76 GISTs, combined with genome-wide mRNA expression analysis in 22 GISTs, to identify signatures associated with clinicopathological parameters and prognosis. Principal component analysis revealed distinct DNA methylation patterns associated with anatomical localization, genotype, mitotic counts and clinical follow-up. Methylation of a single CpG dinucleotide in the non-CpG island promoter of *SPP1* was significantly correlated with shorter disease-free survival. Hypomethylation of this CpG was an independent prognostic parameter in a multivariate analysis compared to anatomical localization, genotype, tumor size and mitotic counts in a cohort of 141 GISTs with clinical follow-up. The epigenetic regulation of SPP1 was confirmed *in vitro*, and the functional impact of SPP1 protein on tumorigenesis-related signaling pathways was demonstrated. In summary, *SPP1* promoter methylation is a novel and independent prognostic parameter in GISTs, and might be helpful in estimating the aggressiveness of GISTs from the intermediate-risk category.

Gastrointestinal stromal tumors (GISTs) are the most common mesenchymal tumors of the gastrointestinal tract, most likely derived from interstitial cells of cajal (ICCs) or their stem cell precursor cells. The initial events in GIST tumorigenesis are gain-of-function mutations of the receptor tyrosine kinases *v-kit Hardy-Zuckerman 4 feline sarcoma viral oncogene homolog* (*KIT*) or *platelet-derived growth factor receptor, alpha polypeptide* (*PDGFRA*), occurring in ~75 and

Key words: GIST, methylation, SPP1
Conflict of interest: Nothing to report
Jitao David Zhang's current address is: Bioinformatics and Exploratory Data Analysis, Pharma Research and Early Development, F. Hoffmann-La Roche AG, Basel, Switzerland.
Özgür Sahin's current address is: Department of Molecular Biology and Genetics, Bilkent University, Ankara, Turkey.
Yasser Riazalhosseini's current address is: McGill University and Genome Quebec Innovation Centre and Department of Human Genetics, McGill University, Montreal, Canada
Grant sponsors: DKFZ International PhD Program, Wilhelm Sander-Stiftung; **Grant sponsor:** National Genome Research Network of the Federal Ministry of Education and Research (BMBF); **Grant numbers:** 01GS0864, 01GS0816
DOI: 10.1002/ijc.29088
History: Received 28 Jan 2014; Accepted 3 July 2014; Online 21 July 2014
Correspondence to: Prof. Dr. med. Florian Haller, Institute of Pathology, Krankenhausstr. 8–10, D-91054 Erlangen, Germany, Tel.: +49-9131-85-25677, Fax: +49-9131-85-25679, E-mail: florian.haller@uk-erlangen.de

What's new?
Variations in the clinical behavior of gastrointestinal stromal tumors (GISTs) are associated with underlying variations in gene expression. But the mechanisms regulating gene expression in GIST and how they influence tumor progression remain unclear. A mechanism implicated in the present study is epigenetic dysregulation, specifically of secreted phosphoprotein 1 (*SPP1*), based on targeted DNA methylation profiling and genome-wide mRNA expression analysis in a cohort of GISTs. *In vitro* experiments indicate that SPP1 raises oncogenic potential by influencing the activation of major intracellular regulators. The findings suggest that *SPP1* hypermethylation is an independent prognostic marker in GIST.

15% of GISTs, respectively.[1,2] The histomorphologic appearance and clinical behavior are significantly different between gastric and small intestinal GISTs,[3,4] and also between GISTs with *KIT* and *PDGFRA* mutations.[5,6] Gastric GISTs and GISTs with *PDGFRA* mutations are associated with less aggressive behavior compared to small intestinal GISTs and to GISTs with *KIT* mutations.[3–6] Array-based genome-wide expression studies have shown significant differences in mRNA expression signatures comparing gastric and small intestinal GISTs,[7,8] GISTs with *KIT* and *PDGFRA* mutations[9,10] and according to risk classification.[8,11] However, little is known about the underlying mechanisms regulating these expression signatures.

Epigenetic regulation by DNA methylation of cytosine residues in CpG dinucleotides silences gene expression by affecting the recruitment of regulatory proteins to DNA,[12] and has been shown to play causal roles in the pathogenesis of several cancers.[13] However, only limited data have been reported concerning epigenetic mechanisms in GIST tumorigenesis and prognosis.[14] Two earlier studies have reported downregulation of the *CDK* inhibitor $p16^{INK4A}$, partly due to promoter hypermethylation of the corresponding gene locus *CDKN2A*, as a prognostic marker for GIST progression.[15,16] Hypomethylation of LINE-1 repeats was found to correlate with risk classification and chromosomal instability.[17] Another study has compared the global DNA methylation patterns in GISTs of different risk categories, and identified *REC8* and *PAX3* to be differentially methylated in small *vs*. malignant GISTs.[18] Epigenetic silencing of the tumor suppressor gene *PTEN* has been found after long-term exposure of GIST tumor cells to sunitinib.[19]

In our study, we performed targeted DNA methylation profiling in a large cohort of primary GISTs and observed distinct methylation patterns according to anatomical localization, genotype and mitotic counts. According to the prognostic value of these factors, we established a linear model to identify DNA methylation events that are associated with tumor progression independently of the classical clinicopathological parameters mentioned above. On the basis of correlation analysis with gene expression and *in vitro* findings, we demonstrate methylation of *Secreted Phosphoprotein 1* (*SPP1*) promoter as a potent regulator of its expression, and highlight *SPP1* promoter hypomethylation as a novel and independent prognostic parameter in GISTs.

Material and Methods

Tumor samples

A cohort of 76 fresh-frozen tumor samples from primary GISTs without previous imatinib treatment was used for targeted DNA methylation analysis (test set). An additional cohort of 99 paraffin-embedded imatinib-naïve primary GISTs was used as the validation set. Clinical follow-up was available for 42 of the 76 fresh-frozen GISTs of the test set, and for all 99 paraffin-embedded GISTs of the validation set. For each tumor, DNA was isolated from fresh-frozen or paraffin-embedded tissue using the Qiagen Mini Kit (Qiagen, Hilden, Germany) according to the manufacturer's manual, and DNA concentration was quantified with a NanoDrop 1000 (Thermo Scientific, Wilmington, DE). Mutation analysis of KIT exons 9, 11, 13 and 17 as well as PDGFRA exons 12, 14 and 18 was performed in all 175 samples using the methods previously described.[20] This study was approved by the ethics committee of the University of Göttingen (No. 8/9/07).

DNA methylation analysis

The 76 GISTs from the test set were analyzed with the Golden Gate Methylation Cancer Panel I (Illumina, San Diego, CA) at 1,505 CpG loci associated with 807 cancer-related genes. DNA methylation patterns of six individual CpG loci in the promoter region of SPP1 were evaluated by bisulfite sequencing in DNA samples from three GISTs with varying levels of SPP1 methylation according to the Golden Gate Methylation data set. After sodium bisulfite treatment using the EpiTect bisulfite Kit (Qiagen), a genomic region upstream of the transcription start site of SPP1 was amplified by polymerase chain reaction (PCR) using the following primers: SPP1_SBF1 AATGTGTAAAATTTTTTTATTGATGTATAT and SPP1_SBR1 ATCCTTTACTACTCAAACTTAACTTTATAA. PCR products were cloned using the TOPO TA cloning kit for sequencing (Invitrogen, Carlsbad, CA), and ten individual clones from each sample were sequenced. Bisulfite pyrosequencing of the most informative SPP1 CpG site (SPP1_P647_F) was performed for all samples. A 73-bp fragment of the SPP1 promoter region was PCR-amplified from bisulfite-treated DNA (EZ DNA Methylation-Gold Kit; Zymo Research, Irvine, CA) using GTATTTTATGGATGAGGGAATAAGGATAG (forward) and ATCACTACTAACCTATACAACCTTAAAC (reverse) primers. Pyrosequencing reactions were done using the PyroMark Gold Q24 Reagents (Qiagen) in a PyroMark Q24 Pyrosequencing System (Qiagen) with the pyrosequencing primer

AGGGAATAAGGATAGGTA. Quantification of CpG methylation was performed using the Software PyroMark 24 v.2.0.6 (Qiagen), with correction for minor bias toward unmethylated alleles as previously described.[21]

mRNA expression analysis

After homogenization of fresh-frozen tumor tissue with an Ultra Turrax T25 (IKA-Werke GmbH), total RNA was isolated with TRIzol Reagent (Invitrogen) and total RNA concentration and integrity was quantified using the Agilent 2100 Bioanalyzer (Agilent Technologies, Palo Alto, CA). Genome-wide mRNA expression analysis was performed for 22 samples of highest RNA integrity using the HumanHT-12 v4 Expression BeadChip Kit (Illumina). cDNA synthesis for quantitative RT-PCR was performed for 51 GISTs of the test set with the Revert-Aid H Minus First Strand cDNA Synthesis Kit (Fermentas, St. Leon-Rot, Germany) using 10 ng of total RNA. The qRT-PCRs for *SPP1* and reference genes *ACTB* and *HPRT* were performed with an ABI Prism 7900HT Sequence Detection System (Applied Biosystems, Weiterstadt, Germany), using probes 61 (for *SPP1*), 64 (for *ACTB*) and 73 (for *HPRT*) of the Universal Probe Library (Roche, Penzberg, Germany), together with the following primers: SPP1_forward CGCAGACCTGACATCCAGTA, SPP1_reverse GGCTGTCCCAATCAGAAGG; ACTB_forward CCAACCGCGAGAAGATGA, ACTB_reverse CCAGAGGCGTACAGGGATAG; HPRT_forward TGACCTTGATTTATTTTGCATACC, HPRT_reverse CGAGCAAGACGTTCAGTCCT. Data were analyzed with the ddCt algorithm (Bioconductor *package ddCt*).

In vitro inhibition of DNA methylation and SPP1 stimulation in GIST cell lines

Cell culture conditions for GIST cell line GIST882 were as described previously.[22] Cells were cultured for 24 hr and then treated with 10 or 25 nM concentrations of 5-aza-2′-deoxycytidine (A3656-5MG, Sigma-Aldrich Chemie GmbH, Munich, Germany) for 72 hr. After treatment, DNA and total RNA were isolated for DNA methylation analysis using pyrosequencing and for mRNA expression analysis using qRT-PCR as described above. Additionally, protein lysates were collected, and Western blot analysis of SPP1 protein levels was performed using a monoclonal anti-SPP1 antibody (LFMb-14, Santa Cruz Biotechnology, Santa Cruz, CA). To examine downstream signaling of SPP1, GIST882 cells were treated with 1 μg recombinant SPP1 after starvation of the cells, and cell lysis was done on ice at different time points (0, 5, 15, 30 and 60 min). Western blot analyses for expression as well as phosphorylation of AKT and ERK1/2 were carried out as described previously.[23]

Statistical analysis

Read-outs from Golden Gate Methylation Cancer Panel I were normalized with *logit*-transformation. Principal components analysis was performed with the ROBPCA algorithm.[24] Differential methylation was detected by establishing a linear model with classical clinical parameters as covariates and by moderated *t*-tests followed by Benjamini & Hochberg adjustment to control false-discovery rate (FDR) under 0.01, as described by the Bioconductor package *limma*.[25] Briefly, for each CpG locus, the logit-transformed methylation value y was fitted to the following model:

$$\gamma \sim \mu + \beta_l l + \beta_g g + \beta_m m + \beta_p p,$$

where μ represents the baseline methylation level, l, g, m and p present factor variables of anatomical localization, genotype, mitotic counts and tumor progression, respectively, and βs represent respective coefficients. By this model, we assume that the methylation status of each CpG locus can be explained by the linear combination of four factors. The linear model was fitted and null hypotheses were tested assuming that the coefficients (βs) equal zero. Benjamini–Hochberg multiple-testing adjustment was performed. All statistical tests were performed with R and Bioconductor,[26] or with SPSS Statistics software (IBM, New York, NY).

Results

Unsupervised targeted DNA methylation analysis classifies GISTs into subgroups correlated to anatomical localization and genotype

A three-dimensional principal component analysis (PCA) was performed to detect distinct patterns in 76 fresh-frozen GIST samples according to the methylation status of 1,505 CpG loci representing 807 cancer-related genes (Fig. 1*a*). Correlation with clinicopathological parameters revealed that the GISTs separated into three distinct groups: gastric with *KIT* mutation; small intestine with *KIT* mutation and gastric with *PDGFRA* mutation. Two rectal GISTs with *KIT* mutation clustered with the gastric *KIT*-mutated GISTs, while three wild-type GISTs clustered according to their anatomical localization (either gastric or small intestinal) among the *KIT*-mutated GISTs. Interestingly, one CpG locus located in the promoter region of the gene *prominin 1* (*PROM1*)/*CD133* as well as two CpG loci located in the promoter region of the gene *CD34 molecule* (*CD34*) displayed a similar methylation pattern, with low methylation levels in *KIT*-mutated GISTs from the stomach and rectum, in contrast to high methylation levels in *KIT*-mutated GISTs from the small intestine (Fig. 1 and Table 1).

The methylation status of distinct CpG loci is associated with anatomical localization, genotype, mitotic counts and tumor progression in GIST

The standard prognostication of clinical behavior in GIST is based on the parameters anatomical localization, size and mitotic counts. Accordingly, novel and additional molecular parameters have to be of independent prognostic value compared to those well-established and easily accessible factors. Thus, we used a linear model to identify CpG loci that give additional prognostic information beyond those classical

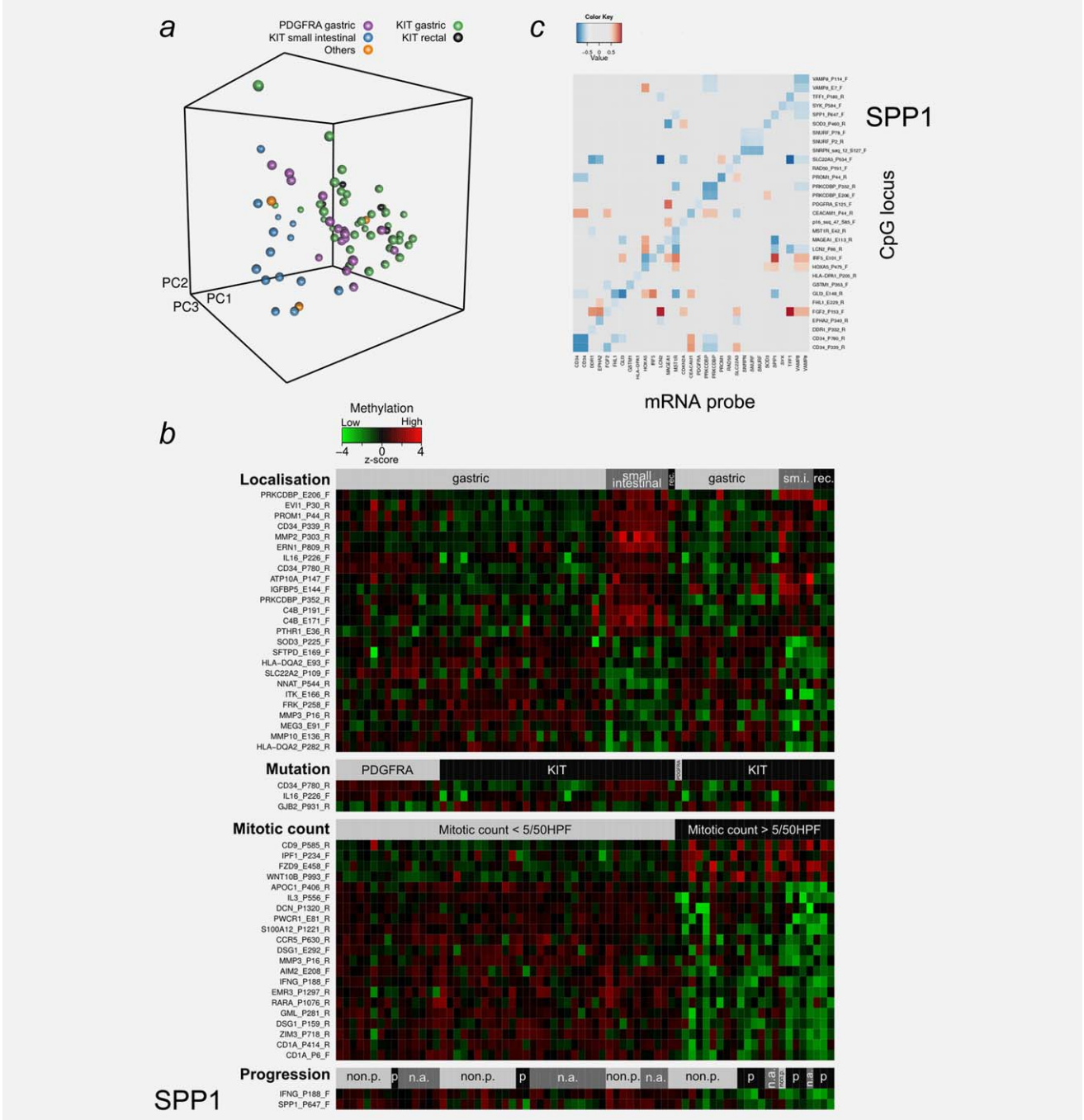

Figure 1. Targeted DNA methylation analysis identified *SPP1* as a novel prognostic factor. (*a*) Unsupervised three-dimensional PCA reveals distinct patterns of DNA methylation in relation to anatomical localization and genotype. There is a clear separation of three distinct groups: *KIT*-mutated GISTs from the stomach (green), *KIT*-mutated GISTs from the small intestine (blue) and *PDGFRA*-mutated GISTs from the stomach (purple). Rectal GISTs (black) cluster with gastric *KIT*-mutated GISTs, and wild-type GISTs (orange) cluster according to their anatomical localization within the *KIT*-mutated tumors. (*b*) Heatmap of differentially methylated CpG loci according to clinicopathological parameters and tumor progression. The linear model revealed a significant association of DNA methylation at specific CpG loci with anatomical localization (25 CpG loci), genotype (three CpG loci), mitotic counts (21 CpG loci) and tumor progression (two CpG loci). Three CpG loci located in the promoter regions of *PROM1*/*CD133* and *CD34* display a similar methylation pattern within GIST from different sites of the gastrointestinal tract. The linear model further demonstrates that hypomethylation of the CpG locus SPP1_P647_F in the promoter region of *SPP1* is independently correlated to tumor progression. Sm. i.: small intestinal; rec.: rectal; non p.: nonprogressive; p.: progressive; n.a.: not available. (*c*) Correlation analysis of DNA methylation (*y*-axis) and genome-wide mRNA expression (*x*-axis) was used to detect 31 CpG loci with significant inverse mRNA expression levels of their respective genes (27), including PROM1/CD133, CD34 and SPP1.

Table 1. Summary of differentially methylated CpG sites in correlation to clinicopathological parameters and follow-up

CpG ID	CpG island	Distance to TSS	Entrez gene ID	Gene symbol	Description	Log fold change	BH-adjusted *p*-value
Localization: stomach *vs*. small intestinum							
PRKCDBP_E206_F	Y	206	112464	PRKCDBP	Protein kinase C, delta binding protein	3.0	7e−09
EVI1_P30_R	Y	−30	2122	MECOM	MDS1 and EVI1 complex locus	2.7	1e−07
PROM1_P44_R	N	−44	8842	PROM1	Prominin 1	2.4	3e−08
CD34_P339_R	N	−339	947	CD34	CD34 molecule	2.1	3e−08
MMP2_P303_R	Y	−303	4313	MMP2	Matrix metallopeptidase 2	1.8	7e−08
ERN1_P809_R	Y	−809	2081	ERN1	Endoplasmic reticulum to nucleus signaling 1	1.6	5e−06
IL16_P226_F	N	−226	3603	IL16	Interleukin 16	1.5	0.0002
CD34_P780_R	N	−780	947	CD34	CD34 molecule	1.5	0.0001
ATP10A_P147_F	Y	−147	57194	ATP10A	ATPase, class V, type 10A	1.4	4e−05
IGFBP5_E144_F	Y	144	3488	IGFBP5	Insulin-like growth factor binding protein 5	1.3	5e−06
PRKCDBP_P352_R	Y	−352	112464	PRKCDBP	Protein kinase C, delta binding protein	1.3	0.0002
C4B_P191_F	N	−191	721	C4B	C4B	1.0	0.0003
C4B_E171_F	N	171	721	C4B	C4B	0.9	4e−05
PTHR1_E36_R	N	36	5745	PTH1R	Parathyroid hormone 1 receptor	0.9	0.0002
SOD3_P225_F	N	−225	6649	SOD3	Superoxide dismutase 3, extracellular	−0.5	0.0002
SFTPD_E169_F	N	169	6441	SFTPD	Surfactant protein D	−0.6	0.0002
HLA-DQA2_E93_F	N	93	3118	HLA-DQA2	Major histocompatibility complex, class II, DQ alpha 2	−0.7	0.0003
SLC22A2_P109_F	Y	−109	6582	SLC22A2	SLC22A2	−0.8	3e−05
NNAT_P544_R	Y	−544	4826	NNAT	Neuronatin	−1.1	1e−06
ITK_E166_R	N	166	3702	ITK	IL2-inducible T-cell kinase	−1.1	7e−05
FRK_P258_F	N	−258	2444	FRK	fyn-related kinase	−1.2	0.0002
MMP3_P16_R	N	−16	4314	MMP3	Matrix metallopeptidase 3	−1.2	5e−05
MEG3_E91_F	Y	91	55384	MEG3	MEG3	−1.3	0.0003
MMP10_E136_R	N	136	4319	MMP10	Matrix metallopeptidase 10	−1.3	0.0002
HLA-DQA2_P282_R	N	−282	3118	HLA-DQA2	Major histocompatibility complex, class II, DQ alpha 2	−1.3	4e−08

Table 1. Summary of differentially methylated CpG sites in correlation to clinicopathological parameters and follow-up (Continued)

CpG ID	CpG island	Distance to TSS	Entrez gene ID	Gene symbol	Description	Log fold change	BH-adjusted *p*-value
Genotype: *KIT* mutation *vs.* *PDGFRA* mutation							
CD34_P780_R	N	−780	947	CD34	CD34 molecule	1.9	6e−06
IL16_P226_F	N	−226	3603	IL16	Interleukin 16	1.6	0.0003
GJB2_P931_R	Y	−931	2706	GJB2	Gap junction protein, beta 2, 26 kDa	−1.8	0.0001
Mitotic counts: low (<5/50 HPFs) *vs.* high (>5/50 HPFs) mitotic counts							
CD9_P585_R	Y	−585	928	CD9	CD9 molecule	1.3	7e−05
IPF1_P234_F	Y	−234	3651	PDX1	Pancreatic and duodenal homeobox 1	1.2	3e−05
FZD9_E458_F	Y	458	8326	FZD9	Frizzled homolog 9	1.1	0.0003
WNT10B_P993_F	Y	−993	7480	WNT10B	Wingless-type MMTV integration site family, member 10B	1.0	8e−05
APOC1_P406_R	Y	−406	341	APOC1	Apolipoprotein C-I	−0.3	0.0003
IL3_P556_F	N	−556	3562	IL3	Interleukin 3	−0.5	2e−05
DCN_P1320_R	N	−1320	1634	DCN	Decorin	−0.5	0.0001
PWCR1_E81_R	N	81	727708	SNORD116-19	Small nucleolar RNA, C/D box 116-19	−0.7	0.0002
S100A12_P1221_R	N	−1221	6283	S100A12	S100 calcium binding protein A12	−0.7	5e−06
CCR5_P630_R	N	−630	1234	CCR5	Chemokine (C-C motif) receptor 5	−0.8	7e−05
DSG1_E292_F	N	292	1828	DSG1	Desmoglein 1	−1.0	0.0002
MMP3_P16_R	N	−16	4314	MMP3	Matrix metallopeptidase 3	−1.1	0.0004
AIM2_E208_F	N	208	9447	AIM2	Absent in melanoma 2	−1.1	0.0002
IFNG_P188_F	N	−188	3458	IFNG	Interferon, gamma	−1.1	4e−05
EMR3_P1297_R	Y	−1297	84658	EMR3	EMR3	−1.1	0.0003
RARA_P1076_R	N	−1076	5914	RARA	Retinoic acid receptor, alpha	−1.1	6e−05
GML_P281_R	N	−281	2765	GML	Glycosylphosphatidylinositol anchored molecule-like protein	−1.2	6e−05
DSG1_P159_R	N	−159	1828	DSG1	Desmoglein 1	−1.3	0.0002
ZIM3_P718_R	N	−718	114026	ZIM3	Zinc finger, imprinted 3	−1.3	8e−06
CD1A_P414_R	N	−414	909	CD1A	CD1a molecule	−1.4	0.0002
CD1A_P6_F	N	−6	909	CD1A	CD1a molecule	−1.8	3e−06
Follow-up: no progression *vs.* progression							
IFNG_P188_F	N	−188	3458	IFNG	Interferon, gamma	−1.2	0.0001
SPP1_P647_F	N	−647	6696	SPP1	Secreted phosphoprotein 1	−1.5	0.0003

Abbreviation: TSS: transcription start site.

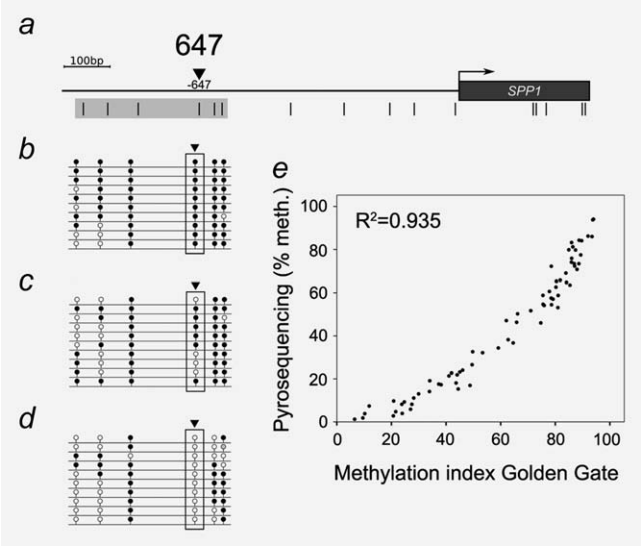

Figure 2. Bisulfite sequencing of the promoter region of *SPP1* confirmed strongest regulation of CpG at position 647, and pyrosequencing validated methylation levels of SPP1 compared to Illumina Golden Gate data. (*a*) Overview of the *SPP1* promoter region. The dark gray box on the right and the bent arrow represent the first exon of *SPP1* and the transcription start site, respectively. The light gray box on the left represents the PCR amplicon used for bisulfite sequencing, comprising six CpG loci. CpG dinucleotides are depicted as vertical lines, and the black arrowhead highlights the CpG site SPP1_P647_F interrogated with the Golden Gate Methylation Cancer Panel I. (*b–d*) Bisulfite sequencing of six CpG loci in three representative GIST samples with high (*b*), intermediate (*c*) and low (*d*) methylation levels according to the Illumina Golden Gate data set. Each line represents an individual clone: closed and open circles represent methylated and unmethylated cytosines, respectively. (*e*) SPP1 methylation level comparing pyrosequencing (*y*-axis) and Illumina Golden Gate reveals a significant correlation ($R^2 = 0.935$).

factors. To achieve this, the linear model calculates for any CpG locus whether its methylation level is correlated to any of the parameters, anatomical localization, size and mitotic counts, and whether a potential prognostic value of its methylation level is dependent or independent of those parameters. This linear model was applied to the methylation status of 1,505 CpG loci in 42 fresh-frozen GIST samples from the test set with clinical follow-up. According to the linear model, 25 CpG loci (22 genes) were associated with anatomical localization, three CpG loci (three genes) with genotype and 21 CpG loci (19 genes) with mitotic counts (Table 1 and Fig. 1*b*). Furthermore, the linear model revealed that methylation patterns in the promoter regions of the two genes *SPP1* and *IFNG* were significantly associated with tumor progression, independently of the clinicopathological parameters described above.

Genome-wide mRNA expression analysis identifies genes with significant inverse correlation between DNA methylation and mRNA expression

To determine if GIST-specific DNA methylation could contribute to distinct gene expression patterns, the levels of DNA methylation at 1.505 CpG dinucleotides were correlated to the mRNA expression levels of the respective genes using genome-wide mRNA expression data for a representative sample of 22 GIST specimens with highest RNA integrity. Given a limited number (807) of cancer-related genes that were interrogated for methylation analyses, this number of GIST samples sufficed for consistent conclusions. Thirty-one CpG loci corresponding to 27 genes were found to have a significant inverse correlation of DNA methylation and mRNA expression (Fig. 1*c*). While *PROM1/CD133*, *CD34* and *SPP1* were among those genes with significant inverse correlation, *IFNG* was not. Bisulfite sequencing of a large portion of the promoter region of *SPP1* in three representative GIST samples with low, intermediate and high *SPP1* methylation levels according to the Illumina Golden Gate Methylation data set revealed strongest regulation of the non-CpG island CpG dinucleotide located 647 base pairs upstream of the transcription start site of *SPP1* that was also represented on the array (Figs. 2*a* and 2*d*). Pyrosequencing of this CpG site in all 76 fresh-frozen GIST samples confirmed the initial methylation levels of the Golden Gate Methylation data set (Fig. 2*e*; $R^2 = 0.94$). SPP1 mRNA expression was further examined by qRT-PCR in 51 of the 76 fresh-frozen GIST samples, revealing a significant inverse correlation between *SPP1* DNA methylation determined by pyrosequencing and SPP1 mRNA expression determined by qRT-PCR ($R^2 = -0.50$).

SPP1 promoter hypomethylation is an independent prognosticator for shorter disease-free survival in GISTs

Using univariate Cox proportional hazard models, a significant correlation was established between hypomethylation of the non-island CpG site 647 base pairs upstream of the transcription start site of *SPP1* and shorter disease-free survival. This significant correlation was observed both in the initial test set of fresh-frozen GIST samples with determination of methylation level using the Illumina Golden Gate method ($p = 0.002$), and also in the validation set of paraffin-embedded GIST samples with determination of methylation levels using pyrosequencing ($p = 0.006$). Accordingly, univariate and multivariate Cox proportional hazard models comparing (*i*) anatomical localization, (*ii*) genotype, (*iii*) tumor size, (*iv*) mitotic counts and (*v*) *SPP1* methylation level determined by pyrosequencing were performed for the whole cohort of 141 samples with clinical follow-up (Table 2). Notably, *SPP1* methylation level remained as an independent prognostic parameter in the multivariate analysis (Table 2). For Kaplan–Meier plot visualization of disease-free survival according to *SPP1* methylation status, the GIST samples were grouped into three groups with low (<25%), intermediate (25–75%) and high (>75%) methylation levels of *SPP1* (Fig. 3), demonstrating the high correlation of this single methylation site with disease progression.

On an individual basis, GISTs of the high-risk category were observed with high *SPP1* methylation levels, which

Table 2. Univariate and multivariate analyses of clinicopathological parameters and *SPP1* methylation status in the whole cohort of 141 GIST samples

Parameter	Univariate analysis (*p*-value)	Multivariate analysis (*p*-value)
Anatomical localization	0.02	0.06
Genotype	0.1	0.9
Tumor size	2.5×10^{-5}	0.003
Mitotic counts	5.5×10^{-11}	0.00004
SPP1 methylation	6.6×10^{-5}	0.03

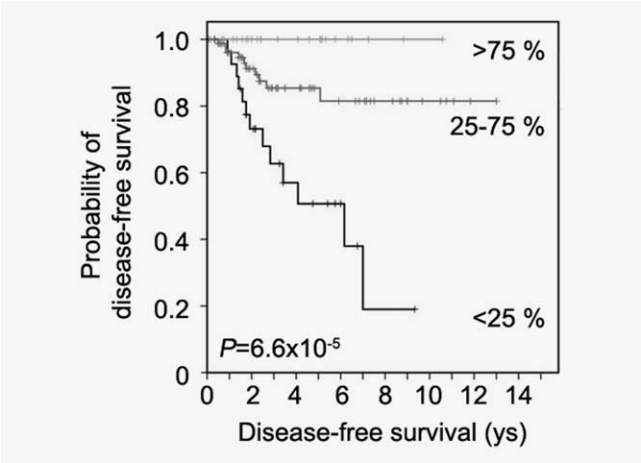

Figure 3. Prognostic impact of *SPP1* methylation determined by pyrosequencing in 141 primary GISTs, comparing tumors with low (<25%), intermediate (25–75%) and high (>75%) methylation levels (univariate Cox proportional hazards model, $p = 6.6 \times 10^{-5}$).

still had a favorable clinical outcome. For example, the highest methylation level (89.9%) was observed in a GIST from the small intestine with >10 mitoses/50 HPFs, which did not progress during a follow-up of 87 months followed by death of another cause. Regarding the only two GISTs among the intermediate-risk category that developed tumor progression, one had lowest methylation levels of only 4%, and the other one had intermediate methylation levels of 41%. Although only limited conclusion can be drawn from these individual cases, they support the independent prognostic role of *SPP1* methylation levels observed for the whole study cohort.

SPP1 expression is correlated with its methylation level *in vitro*, and has stimulating effects on GIST signaling pathways

To evaluate whether the observed correlation between SPP1 methylation and expression levels could be reproduced also *in vitro*, we treated the GIST cell line GIST882 with different concentrations of the demethylating agent 5-aza-2′-deoxycytidine (decitabine) and quantified the mRNA and protein levels of SPP1. Decitabine treatment resulted in a decrease in *SPP1* methylation accompanied by a dose-dependent increase of SPP1 mRNA expression after 72 hr of treatment (Figs. 4*a* and 4*b*). Protein level of SPP1 was increased with the 10 nM decitabine concentration and stayed constant at 25 nM, potentially indicating saturation at protein level (Figs. 4*c* and 4*d*). Furthermore, stimulation of GIST882 cells with 1 μg of recombinant SPP1 induced phosphorylation of ERK1/2 and, to a lesser extent, also of AKT, components of major oncogenic pathways downstream of SPP1 (Fig. 4*e*). Overall, these *in vitro* data support our observations for both SPP1 epigenetic regulation and oncogenic importance of SPP1 modulation in GIST.

Discussion

We performed a targeted DNA methylation profiling analysis of GISTs, revealing distinct patterns according to anatomical localization, genotype and mitotic counts. Applying unsupervised machine learning techniques (PCA), GISTs were separated into three main subgroups: gastric with *KIT* mutation, gastric with *PDGFRA* mutation and small intestinal with *KIT* mutation. Notably, these three GIST subgroups are also characterized by different patterns of mRNA and miRNA expression,[7–11,27] and have distinctive histomorphology and clinical behavior.[3–6] Accordingly, the DNA methylation patterns identified in this study likely represent specific methylation signatures for these three GIST subgroups, which might impact the respective mRNA and miRNA expression patterns, as well as their clinical behavior. Notably, only three genes were differentially methylated in gastric GISTs with *KIT vs*. *PDGFRA* mutations. By contrast, extensive differences in DNA methylation signatures were demonstrated between *KIT*-mutated *GISTs* in the stomach *vs*. small intestine, with differential methylation at 25 CpG loci corresponding to 22 genes. This observation suggests that distinct patterns of epigenetic alterations may be involved in GISTs according to their anatomical origin. Among other genes, the hematopoietic stem cell antigen *PROM1/CD133* was hypomethylated in gastric GISTs, which correlates to its upregulated expression.[28] Interestingly, rectal GISTs with *KIT* mutation clustered together with *KIT*-mutated GISTs from the stomach, consistent with a similar observation based on mRNA expression profiles.[7] This close relationship based on epigenetic and genetic features is in line with the findings that rectal GISTs are predominantly of spindle cell type and uniformly coexpress CD117 and CD34, similar to *KIT*-mutated gastric GISTs of the spindle cell type.[29] Correspondingly, two CpG dinucleotides located in the promoter region of *CD34* showed a distinct methylation pattern among GISTs from different sites of the gastrointestinal tract, with low methylation levels among *KIT*-mutated GISTs from the stomach and rectum in contrast to high methylation levels in *KIT*-mutated GISTs from the small intestine. Notably, both *PROM1/CD133* and *CD34* were among the genes with a significant inverse correlation between DNA methylation and mRNA expression levels in this study. There is accumulating evidence that GISTs arise from ICCs or their stem cell precursor cells, and it has

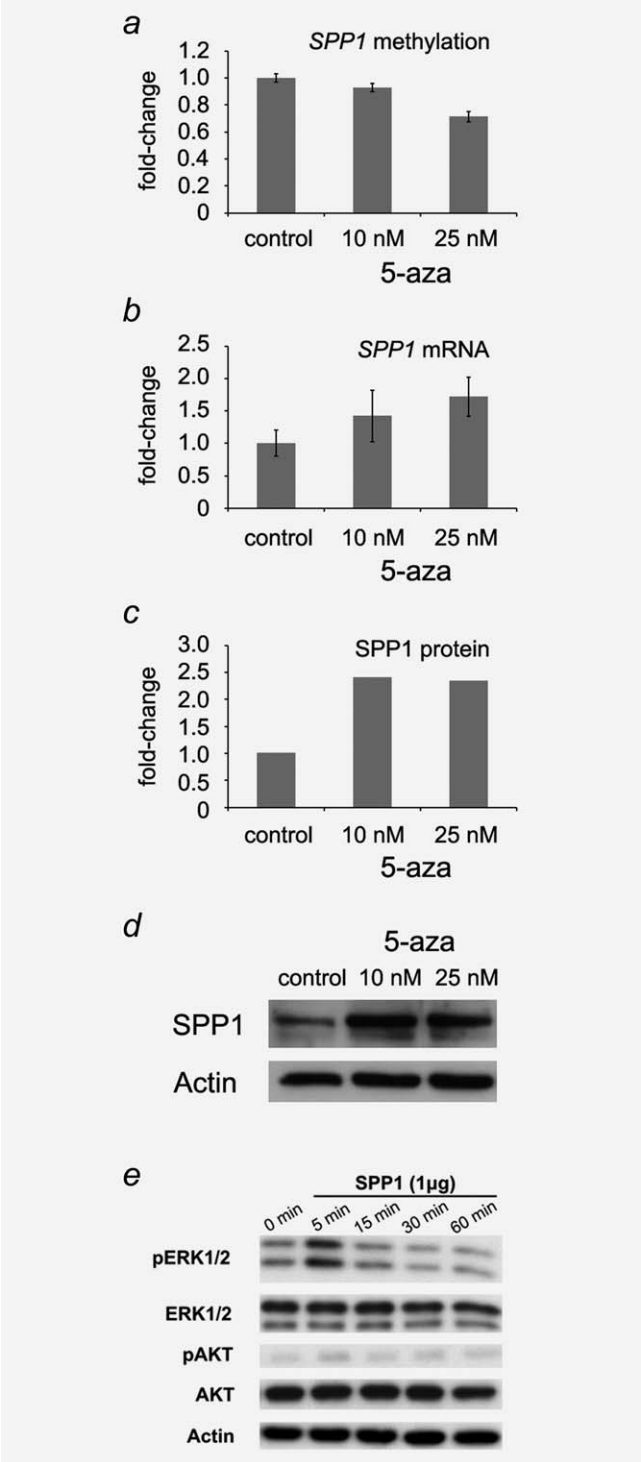

Figure 4. SPP1 mRNA and protein expression levels are inversely correlated to DNA methylation after decitabine treatment *in vitro*, and SPP1 activates intracellular signaling cascades in GIST882 cells. (*a*) *SPP1* methylation levels decreased, while SPP1 mRNA expression (*b*) and SPP1 protein levels (*c*, *d*) increased after treatment of GIST882 cells with increasing doses of DNA methylation inhibitor (5-aza-2′-deoxycytidine or decitabine) for 72 hr. (*e*) Stimulation of GIST882 cells with 1 µg of recombinant SPP1 resulted in an increased phosphorylation of ERK1/2 and AKT with different peaks of activation time.

been shown that at least four different subpopulations of ICCs exist, which have a specific distribution in the gastrointestinal tract.[30] The distinctive DNA methylation patterns including CpG sites within the promoter regions of *PROM1/CD133* and *CD34* that we report for GISTs from different sites of the gastrointestinal tract suggest that varying methylation profiles might underlie the gene expression differences reported for GISTs in these locations, and perhaps reflect the different origins of these GIST subgroups from different ICC-lineage subpopulations.

To identify novel and independent prognostic markers, a linear model comparing classical clinicopathological parameters and follow-up was used to identify CpG sites differentially methylated between GISTs with and without subsequent tumor progression independent of classical prognostic parameters. Additionally, genome-wide mRNA expression analyses were used to establish CpG loci with significant inverse correlation of DNA methylation and mRNA expression, focusing on non-CpG island CpG sites with probable impact on transcription factor binding when compared to probably more global patterns of DNA methylation deregulation frequently observed during tumor progression. This focused approach identified hypomethylation of a CpG dinucleotide 647 base pairs upstream of the transcription start site of *SPP1* to be significantly associated with tumor progression, with inverse correlation to SPP1 mRNA expression. SPP1 is a chemokine-like, acidic glycoprotein that is secreted into the extracellular matrix and that binds certain CD44 variants (*e.g.*, CD44v6) and integrin receptors (*e.g.*, $\alpha_v\beta_3$).[31] SPP1 binding leads to the activation of major intracellular signaling regulators, including PI3K/AKT and RAS/MAPK, thereby effecting the oncogenic potential by promoting proliferation, survival, migration and angiogenesis.[32–34] Noteworthy, PI3K/AKT and RAS/MAPK are the main activated signaling pathways in GIST.[35,36] Using an *in vitro* model, we observed that treatment of GIST882 cells with the demethylating drug decitabine resulted in a dose-dependent downregulation of *SPP1* methylation that was accompanied by an upregulation of SPP1 mRNA as well as protein, supporting the relevance of epigenetic regulation on SPP1 expression in GISTs. Moreover, stimulation of GIST882 cells with SPP1 resulted in the activation of signaling intermediates ERK1/2 and, to a lesser extent, AKT. Altogether, these *in vitro* findings suggest that hypomethylation of *SPP1* and the resulting increase in SPP1 expression may lead to an activation of downstream signaling components with potential impact on proliferation and invasion in GISTs. Notably, the independent prognostic impact of *SPP1* methylation levels with respect to mitotic counts further highlights invasion as a potentially relevant but yet not well-understood mechanism of tumor progression in GIST.

SPP1 (osteopontin) has been demonstrated to be a prognostic marker on the protein level in different kinds of cancers[37–39] and also in GISTs.[40,41] Comparing two different methods and two different GIST cohorts, we established and

validated *SPP1* methylation level as an excellent prognostic factor in GISTs. Using the whole cohort of 141 GISTs with long-term follow-up, *SPP1* methylation level remained an independent prognostic factor in a multivariate analysis compared to anatomic localization, tumor size and mitotic counts. Notably, these three parameters are the best predictors of GIST behavior to date, and they are the basis for the currently used GIST risk classifications.[42,43] Regarding the independent prognostic value of *SPP1* in comparison to these clinicopathological parameters, we suggest that determination of *SPP1* methylation might be especially valuable in GISTs of the intermediate-risk categories, for which the clinical behavior is currently unpredictable. In contrast to the already suggested prognostic role of semiquantitative evaluation of SPP1 protein levels,[40,41] the analysis of *SPP1* methylation degree has the advantage to be a quantitative parameter, with highest sensitivity and reproducibility, and may be easier to implement into GIST risk classifications in the future. Given the fact that DNA analysis by pyrosequencing is now being routinely performed at many diagnostic molecular pathology laboratories, quantification of *SPP1* methylation can be easily established at different laboratories, which is opposed to more complex molecular prognostication schemes that remain restricted to specialized laboratories.[44]

Acknowledgements

The authors thank Sara Burmester, Claudia Köbele, Christian Schmidt and Stefanie Schwager for excellent technical assistance. They acknowledge the DKFZ Genomics and Proteomics Core Facility for performing excellent services. J.D.Z. was supported by the DKFZ International PhD Program. S.W. was supported within the National Genome Research Network (grants 01GS0864 and 01GS0816) of the Federal Ministry of Education and Research (BMBF). O.S. and S.W. were further supported by the Wilhelm Sander-Stiftung. F.H. and O.S. conceived the study design and experiments, analyzed data and wrote the manuscript. E.A.M., A.Br., Y.R., A.W., A.Ba. and B.K. carried out experiments. J.D.Z., B.K., J.H. and S.W. analyzed data. I.M.S., S.C., B.M.G., C.O., H.G., M.W., A.A., A.H. and J.A.F. were involved in the study design and contributed to data collection. All authors were involved in writing the paper and had final approval of the submitted and published versions.

References

1. Hirota S, Isozaki K, Moriyama Y, et al. Gain-of-function mutations of c-kit in human gastrointestinal stromal tumors. *Science* 1998;279:577–80.
2. Heinrich MC, Corless CL, Duensing A, et al. PDGFRA activating mutations in gastrointestinal stromal tumors. *Science* 2003;299:708–10.
3. Miettinen M, Sobin LH, Lasota J. Gastrointestinal stromal tumors of the stomach: a clinicopathologic, immunohistochemical, and molecular genetic study of 1765 cases with long-term follow-up. *Am J Surg Pathol* 2005;29:52–68.
4. Miettinen M, Makhlouf H, Sobin LH, et al. Gastrointestinal stromal tumors of the jejunum and ileum: a clinicopathologic, immunohistochemical, and molecular genetic study of 906 cases before imatinib with long-term follow-up. *Am J Surg Pathol* 2006;30:477–89.
5. Wardelmann E, Hrychyk A, Merkelbach-Bruse S, et al. Association of platelet-derived growth factor receptor alpha mutations with gastric primary site and epithelioid or mixed cell morphology in gastrointestinal stromal tumors. *J Mol Diagn* 2004;6:197–204.
6. Lasota J, Dansonka-Mieszkowska A, Sobin LH, et al. A great majority of GISTs with PDGFRA mutations represent gastric tumors of low or no malignant potential. *Lab Invest* 2004;84:874–83.
7. Antonescu CR, Viale A, Sarran L, et al. Gene expression in gastrointestinal stromal tumors is distinguished by KIT genotype and anatomic site. *Clin Cancer Res* 2004;10:3282–90.
8. Yamaguchi U, Nakayama R, Honda K, et al. Distinct gene expression-defined classes of gastrointestinal stromal tumor. *J Clin Oncol* 2008;26:4100–8.
9. Subramanian S, West RB, Corless CL, et al. Gastrointestinal stromal tumors (GISTs) with KIT and PDGFRA mutations have distinct gene expression profiles. *Oncogene* 2004;23:7780–90.
10. Kang HJ, Nam SW, Kim H, et al. Correlation of KIT and platelet-derived growth factor receptor alpha mutations with gene activation and expression profiles in gastrointestinal stromal tumors. *Oncogene* 2005;24:1066–74.
11. Koon N, Schneider-Stock R, Sarlomo-Rikala M, et al. Molecular targets for tumour progression in gastrointestinal stromal tumours. *Gut* 2004;53:235–40.
12. Sharma S, Kelly TK, Jones PA. Epigenetics in cancer. *Carcinogenesis* 2010;31:27–36.
13. Feinberg AP, Tycko B. The history of cancer epigenetics. *Nat Rev Cancer* 2004;4:143–53.
14. Sioulas AD, Vasilatou D, Pappa V, et al. Epigenetics in gastrointestinal stromal tumors: clinical implications and potential therapeutic perspectives. *Dig Dis Sci* 2013;58:3094–3102.
15. Schneider-Stock R, Boltze C, Lasota J, et al. High prognostic value of p16INK4 alterations in gastrointestinal stromal tumors. *J Clin Oncol* 2003;21:1688–97.
16. Ricci R, Arena V, Castri F, et al. Role of p16/INK4a in gastrointestinal stromal tumor progression. *Am J Clin Pathol* 2004;122:35–43.
17. Igarashi S, Suzuki H, Niinuma T, et al. A novel correlation between LINE-1 hypomethylation and the malignancy of gastrointestinal stromal tumors. *Clin Cancer Res* 2010;16:5114–23.
18. Okamoto Y, Sawaki A, Ito S, et al. Aberrant DNA methylation associated with aggressiveness of gastrointestinal stromal tumour. *Gut* 2012;61:392–401.
19. Yang J, Ikezoe T, Nishioka C, et al. Long-term exposure of gastrointestinal stromal tumor cells to sunitinib induces epigenetic silencing of the PTEN gene. *Int J Cancer* 2012;130:959–66.
20. Haller F, Gunawan B, von Heydebreck A, et al. Prognostic role of E2F1 and members of the CDKN2A network in gastrointestinal stromal tumors. *Clin Cancer Res* 2005;11:6589–97.
21. Moskalev EA, Zavgorodnij MG, Majorova SP, et al. Correction of PCR-bias in quantitative DNA methylation studies by means of cubic polynomial regression. *Nucleic Acids Res* 2011:39:e77.
22. Bauer S, Duensing A, Demetri GD, et al. KIT oncogenic signaling mechanisms in imatinib-resistant gastrointestinal stromal tumor: PI3-kinase/AKT is a crucial survival pathway. *Oncogene* 2007;26:7560–8.
23. Uhlmann S, Zhang JD, Schwäger A, et al. miR-200bc/429 cluster targets PLCgamma1 and differentially regulates proliferation and EGF-driven invasion than miR-200a/141 in breast cancer. *Oncogene* 2010;29:4297–4306.
24. Hubert M, Rousseeuw PJ, Vanden Branden K. ROBPCA: a new approach to robust principal components analysis. *Technometrics* 2005;47:64–79.
25. Smyth GK. Linear models and empirical Bayes methods for assessing differential expression in microarray experiments. *Stat Appl Genet Mol Biol* 2004;3:3.
26. Gentleman RC, Carey VJ, Bates DM, et al. Bioconductor: open software development for computational biology and bioinformatics. *Genome Biol* 2004;5:R80.
27. Haller F, von Heydebreck A, Zhang JD, et al. Localization- and mutation-dependent microRNA (miRNA) expression signatures in gastrointestinal stromal tumours (GISTs), with a cluster of co-expressed miRNAs located at 14q32.31. *J Pathol* 2010;220:71–86.
28. Arne G, Kristiansson E, Nerman O, et al. Expression profiling of GIST: CD133 is associated with KIT exon 11 mutations, gastric location and poor prognosis. *Int J Cancer* 2011;129:1149–61.
29. Miettinen M, Furlong M, Sarlomo-Rikala M, et al. Gastrointestinal stromal tumors, intramural leiomyomas, and leiomyosarcomas in the rectum and anus: a clinicopathologic, immunohistochemical, and molecular genetic study of 144 cases. *Am J Surg Pathol* 2001;25:1121–33.
30. Streutker CJ, Huizinga JD, Driman DK, et al. Interstitial cells of Cajal in health and disease. Part I: normal ICC structure and function with associated motility disorders. *Histopathology* 2007;50:176–89.
31. Rangaswami H, Bulbule A, Kundu GC. Osteopontin: role in cell signaling and cancer progression. *Trends Cell Biol* 2006;16:79–87.

32. Dai J, Peng L, Fan K, et al. Osteopontin induces angiogenesis through activation of PI3K/AKT and ERK1/2 in endothelial cells. *Oncogene* 2009; 28:3412–22.
33. Lin YH, Yang-Yen HF. The osteopontin-CD44 survival signal involves activation of the phosphatidylinositol 3-kinase/Akt signaling pathway. *J Biol Chem* 2001;276:46024–30.
34. Chen YJ, Wei YY, Chen HT, et al. Osteopontin increases migration and MMP-9 up-regulation via alphavbeta3 integrin, FAK, ERK, and NF-kappaB-dependent pathway in human chondrosarcoma cells. *J Cell Physiol* 2009;221:98–108.
35. Duensing A, Medeiros F, McConarty B, et al. Mechanisms of oncogenic KIT signal transduction in primary gastrointestinal stromal tumors (GISTs). *Oncogene* 2004;23:3999–4006.
36. Bauer S, Duensing A, Demetri GD, et al. KIT oncogenic signaling mechanisms in imatinib-resistant gastrointestinal stromal tumor: PI3-kinase/AKT is a crucial survival pathway. *Oncogene* 2007;26:7560–8.
37. Kim JH, Skates SJ, Uede T, et al. Osteopontin as a potential diagnostic biomarker for ovarian cancer. *JAMA* 2002;287:1671–9.
38. Dai N, Bao Q, Lu A, et al. Protein expression of osteopontin in tumor tissues is an independent prognostic indicator in gastric cancer. *Oncology* 2007;72:89–96.
39. Rohde F, Rimkus C, Friederichs J, et al. Expression of osteopontin, a target gene of de-regulated Wnt signaling, predicts survival in colon cancer. *Int J Cancer* 2007;121:1717–23.
40. Hsu KH, Tsai HW, Lin PW, et al. Clinical implication and mitotic effect of CD44 cleavage in relation to osteopontin/CD44 interaction and dysregulated cell cycle protein in gastrointestinal stromal tumor. *Ann Surg Oncol* 2010;17:2199–212.
41. Hsu KH, Tsai HW, Lin PW, et al. Osteopontin expression is an independent adverse prognostic factor in resectable gastrointestinal stromal tumor and its interaction with CD44 promotes tumor proliferation. *Ann Surg Oncol* 2010;17:3043–52.
42. Fletcher CD, Berman JJ, Corless C, et al. Diagnosis of gastrointestinal stromal tumors: a consensus approach. *Hum Pathol* 2002;33:459–65.
43. Miettinen M, Lasota J. Gastrointestinal stromal tumors: review on morphology, molecular pathology, prognosis, and differential diagnosis. *Arch Pathol Lab Med* 2006;130:1466–78.
44. Lagarde P, Pérot G, Kauffmann A, et al. Mitotic checkpoints and chromosome instability are strong predictors of clinical outcome in gastrointestinal stromal tumors. *Clin Cancer Res* 2012;18: 826–38.